Creep of three-phase alloy Fe-30%Al-5.2%Zr

F. Dobeš[1]*, P. Kratochvíl[2], P. Kejzlar[3]

[1] *Institute of Physics of Materials, Academy of Sciences of the Czech Republic, Žižkova 22, 616 62 Brno, Czech Republic*
[2] *Department of Physics of Materials, Faculty of Mathematics and Physics, Charles University in Prague,*
Ke Karlovu 5, 121 16 Praha 2, Czech Republic
[3] *Department of Material Science, Faculty of Mechanical Engineering, Technical University in Liberec,*
Studentská 2, 461 17 Liberec, Czech Republic

Abstract

Compressive creep of alloy based on Fe-30at.%Al with addition of 5.2 at.% zirconium was studied at temperatures from 650 to 900 °C. The alloy was tested in two different states: (i) cast and (ii) annealed at 1000 °C for 50 h. The microstructure of cast alloy consisted of matrix (α/B2/D03) and fine lamellar eutectic composed of λ_1 and (α/B2/D03). The eutectic decomposed during annealing at 1000 °C into λ_1 and τ_1 phases. Stress exponents and activation energies were estimated. The values of the stress exponent n can be explained by dislocation motion controlled by climb. The values of the activation energy in both cast and annealed alloy are greater than the activation enthalpy of diffusion. Creep exposure at 900 °C for about 50 h is probably sufficient for attainment the three-phase structure because the same microstructure was observed after creep at 900 °C, in both as-cast and annealed states. In contrast, creep expositions at 650 and 700 °C did not influence the appearance of microstructure.

K e y   w o r d s: iron aluminides, internal stresses, creep, precipitation

1. Introduction

Alloys based on intermetallic iron and aluminium compounds, Fe$_3$Al and FeAl, are known for their excellent corrosion resistance, relatively low density and cheap input raw materials [1–5]. The main problems that impede their industrial application include low ductility at room temperature and insufficient creep resistance at elevated temperatures. Additions of Zr were found to be beneficial in improving both ductility [4, 6] and creep resistance [7–9]. The influence of small amounts of zirconium, often combined with other elements such as carbon or boron, on mechanical properties of Fe$_3$Al-based alloys was studied in refs. [10–21]. Investigations of larger (i.e., greater than 1 %) zirconium additions to Fe-Al alloys were essentially restricted to flow stress behaviour [22–25]. That is why the influence of the amount of zirconium addition on microstructure, high temperature strength and compressive creep of Fe-30%Al alloys (atomic percent is given throughout this paper) was studied in our previous papers [26, 27].

At aluminium content about 30 %, three-phase equilibrium consisting of α (solid solution of aluminium in iron with body centred cubic lattice), λ_1 (Laves phase (Fe,Al)$_2$Zr) and τ_1 (body centred tetragonal phase with the ThMn$_{12}$-type structure, (Fe,Al)$_{12}$Zr) is observed according to ternary phase diagram [28–30], cf. Fig. 1. With decreasing temperature, three-phase equilibrium changes to two-phase equilibrium ($\alpha + \tau_1$) at lower zirconium concentrations while it persists at zirconium content greater than 4 %. It should be noted that the bcc lattice α changes with decreasing temperature to ordered B2 lattice and finally at temperatures below 496 °C to ordered D0$_3$ lattice [31]. The transition concentrations α-B2 at 0 % Zr correspond to values found by interpolation of transition temperatures redetermined by differential thermal analysis [31]. The purpose of the present paper is to examine in detail creep of the alloy with 30 % of aluminium and 5.2 % of zirconium, i.e.,

*Corresponding author: tel.: +420 532290408; fax: +420 541218657; e-mail address: dobes@ipm.cz
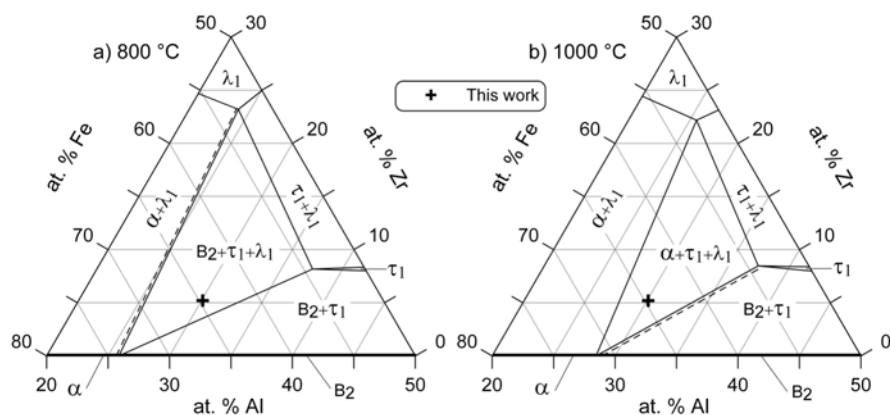
Fig. 1. Details of the isothermal sections of the Fe-Al-Zr ternary diagram at (a) 800 °C and (b) 1000 °C according to Stein et al. [28].

the alloy that conserves its three-phase constitution even at lower temperatures.

2. Experimental methods

The alloy was prepared by melting and casting in a vacuum induction furnace. It contained 64.7 % Fe, 30.1 % Al and 5.2 % Zr. The impurity contents (originating from the raw metals used for the alloy preparation) were determined as 0.1 % Cr, 0.01 % B, 0.1 % Mn and 0.06 % C. Samples prepared from untreated ingots are referred to as "cast". The samples were also annealed at 1000 °C for 50 h in sealed ampoules filled with helium with the aim to stabilize microstructure prior to the creep tests. The annealing was followed by quick cooling in the air outside the furnace. These samples are denoted "annealed". The microstructure after the annealing is expected to be essentially the same as that after the annealing at 1000 °C for 200 h reported in the previous paper [26].

The phase composition and the microstructure were studied by a scanning electron microscope (SEM) equipped with an energy dispersive X-ray analysis system and X-ray diffraction. The volume fractions of the observed phases were evaluated by an analysis of SEM images which were taken in the chemical contrast mode.

Creep tests were performed in uniaxial compression on samples of dimension 12 mm × 5 mm × 5 mm. Samples were prepared by travelling wire electro-discharge machining and fine grinding of surfaces. Tests were performed under a constant load in a protective atmosphere of dry purified argon. The test temperature was held constant within ± 1 K for each individual test. Specimen shortening was measured using a linear variable displacement transducer. The samples were subjected to stepwise loading, where the load changed to a new value after the steady--state creep rate had been established for a given load. Example of time dependence of true compressive
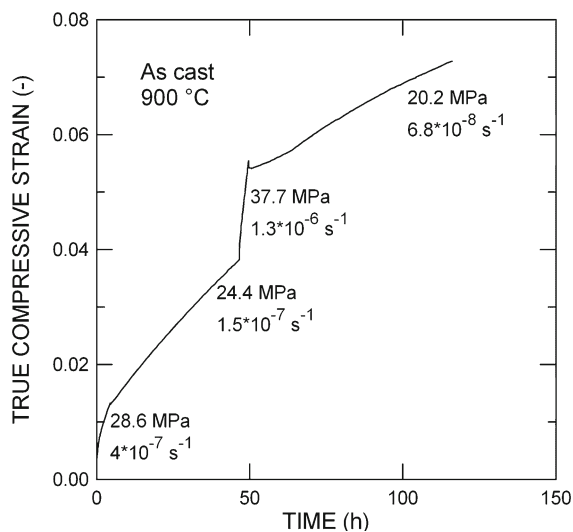

Fig. 2. Example of creep curve obtained in constant-load mode with four loading steps.

strain [32]:

$$\varepsilon = -\ln(l/l_0), \tag{1}$$

where l and l_0 are the instantaneous specimen height and the initial specimen height, respectively, is given in Fig. 2. The terminal values of the true stress [32]:

$$\sigma_i = \frac{F_i l}{S_0 l_0}, \tag{2}$$

where F_i is the force applied in the i-th step and S_0 is the initial cross-section area, and the creep rate, i.e. true compressive strain rate, $\dot{\varepsilon}_i = \mathrm{d}\varepsilon_i/\mathrm{d}t = -(1/l) \cdot \mathrm{d}l/\mathrm{d}t$, were evaluated for each step.

3. Results

Microstructure of nondeformed alloy was documented in the preceding paper [26]. Two types of

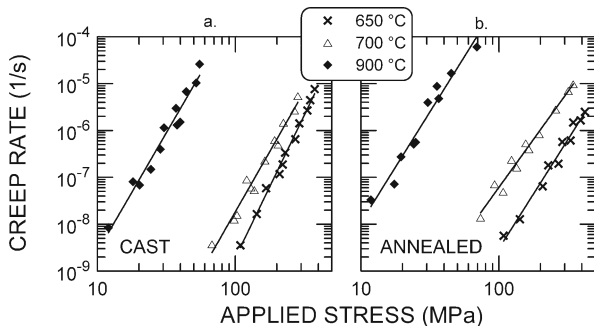Fig. 3. Dependence of the creep rate on the applied stress, separately for cast and annealed alloy at temperatures of 650, 700 and 900 °C.
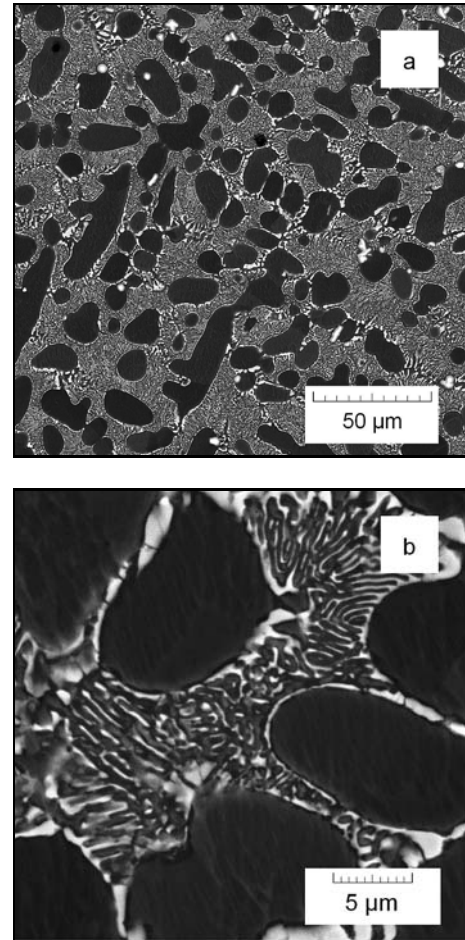

Fig. 4. SEM images of the as-cast alloy after creep at 700 °C in chemical contrast. The dark phase is Fe(Al) (α/B2/D0$_3$), grey areas are eutectic (Fe,Al)$_2$Zr + Fe(Al) (α/B2/D0$_3$), small bright particles are ZrC.

microstructure differing mainly by phase constitution were observed:

(i) The microstructure of as cast alloy consisted of matrix (α/B2/D03) and fine lamellar eutectic composed from λ_1 and (α/B2/D03). The amount of eutectic was determined to be 55.2 %. The constitution corresponds to the as-solidified state predicted by the ternary Fe-Al-Zr phase diagram: the eutectic trough runs nearly parallel to the binary Fe-Al axis at approximately 9–10 % Zr [28].

(ii) The eutectic decomposed during annealing at 1000 °C into λ_1 and τ_1 phases. The volume fractions of the respective phases were: matrix (α/B2/D03) = 46 %, λ_1 = 18.6 % and τ_1 = 35.4 %. This is in agreement with equilibrium phase diagram because three phases (α, λ_1 and τ_1) coexist at temperatures lower than 1130 °C.

The dependences of the creep rate $\dot{\varepsilon}$ on the applied stress σ at the various temperatures for the cast and annealed states are shown in Figs. 3a,b, respectively, on a double logarithmic scale. The data were analyzed using the following relation:

$$\dot{\varepsilon} = A\sigma^n \exp\left(-\frac{Q}{RT}\right), \tag{3}$$

where A is a material constant, n is the stress exponent, Q is the activation energy for creep, R is the gas constant and T is the absolute temperature. The stress exponent and the activation energy were determined by the multiple linear regression. The stress exponent was equal to 5.25 in cast alloy and 4.45 in annealed alloy. A detailed inspection of the data revealed a slight decrease of n with increasing temperature: $n = 6.1$ at 650 °C, 5.1 at 700 °C, and 5.1 at 900 °C in cast alloy and $n = 4.7$ at 650 °C, 4.1 at 700 °C, and 4.7 at 900 °C in annealed alloy.

The activation energy was equal to 430 kJ mol^{-1} in cast alloy and about 420 kJ mol^{-1} in annealed alloy. The obtained values are greater than the activation

enthalpy of diffusion: Activation enthalpy of ^{59}Fe diffusion in Fe-25.5 % Al (B2 lattice) and in Fe-33 % Al (A2/B2 lattice) is equal to 232 and 241 kJ mol^{-1}, respectively [33]. The diffusivity of Al is of a similar magnitude as that of Fe [33, 34]. The above difference between the activation energy of creep and the activation enthalpy of diffusion is typical for Fe-Al alloys. The values ranging from 276 to 418 kJ mol^{-1} are reported for Fe-$\sim$28 % Al alloys in the review paper [4]. It has to be noted that the effect of creep temperature on the microstructure of the alloy makes the interpretation of the activation energy difficult. This objection will be illustrated by the following description of the microstructure after creep tests.

Two types of reaction of microstructure to creep exposition were observed. Creep expositions at 650 and 700 °C did not influence the appearance of microstructure, i.e., the two-phase hypoeutectic microstructure of $\alpha + \lambda_1$ was preserved in as-cast specimens (Fig. 4) and the three-phase transformed microstructure was not changed in annealed specimens
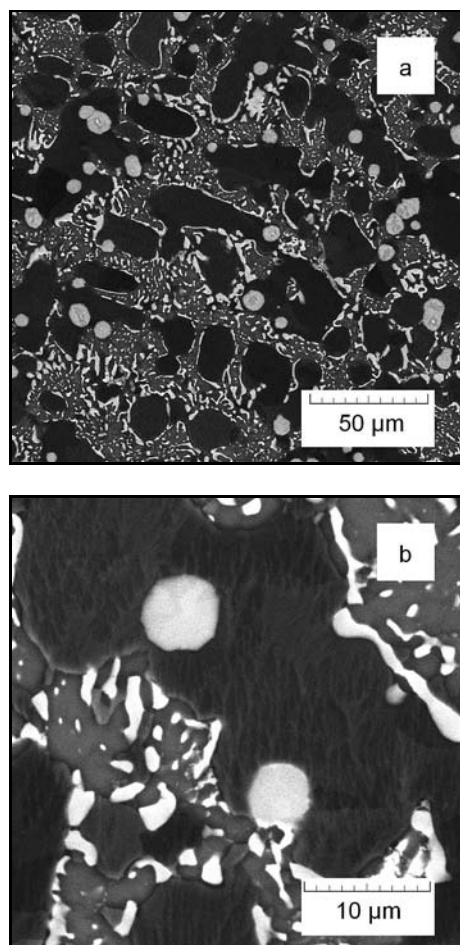
Fig. 5. SEM images of the annealed alloy after creep at $700\,°C$ in chemical contrast: the dark phase is Fe(Al) (α/B2/D0$_3$), grey areas are τ_1-phase (Fe,Al)$_{12}$Zr, bright flakes and round particles are λ_1-Laves phase (Fe,Al)$_2$Zr.

(Fig. 5). On the other hand, the same three-phase microstructure was observed in both cast (Fig. 6) and annealed specimens after creep at $900\,°C$ (Fig. 7). The total holding time at this temperature was about 360 h and about 155 h for cast and for annealed specimen, respectively. To minimize the effect of transition from two-phase to three-phase microstructure during creep of cast sample, creep rates obtained after holding times at the temperature of $900\,°C$ longer than 50 h were taken into account in the evaluation of the stress exponent n.

4. Discussion

Analysis of stress dependence of creep rate by means of level of stress exponent n is a common procedure for estimating mechanisms governing creep processes. The observation of a stress exponent near 5 suggests that the creep rate is controlled by a dislocation climb process as in pure metals and class II
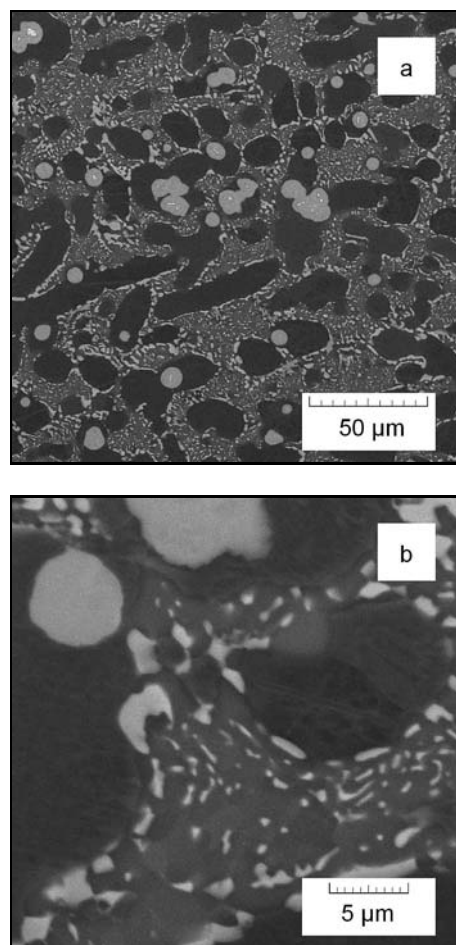
Fig. 6. SEM images of the cast alloy after creep at $900\,°C$.

solid solution alloys [35, 36]. For the complicated alloys of interest, this suggestion can be interpreted as deformation occurs essentially in the Fe(Al) matrix. Particles of λ_1 and τ_1 are coarse and too distant and cannot block the motion of dislocations. The particles thus affect the creep rate through their influence on the distribution of stresses.

A direct comparison of the present results can be done with the recent data on the creep behaviour of Fe-25Al alloys with tantalum additions [37], cf. Fig. 8. The data for both compared alloys were obtained by the same experimental technique and under approximately the same conditions (annealing for 50 h (Zr) and 200 h (Ta) at $1000\,°C$). Creep resistances of alloys with 5.2 % Zr and 2 % Ta at temperature of $700\,°C$ are approximately equal to each other. It should be noted that the difference in weight % is small, 7.08 wt.% Ta vs. 9.68 wt.% Zr.

5. Conclusions

Creep properties of the alloy with 30 at.% Al and 5.2 at.% Zr were studied at temperatures from 650 to
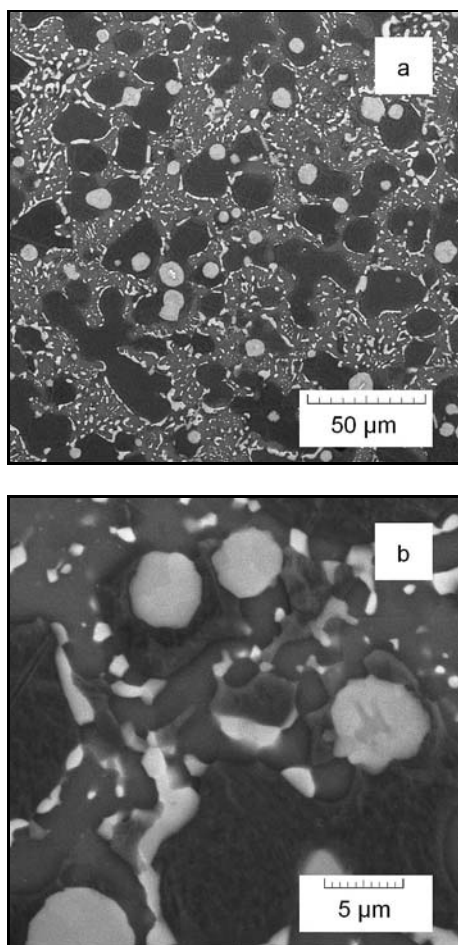
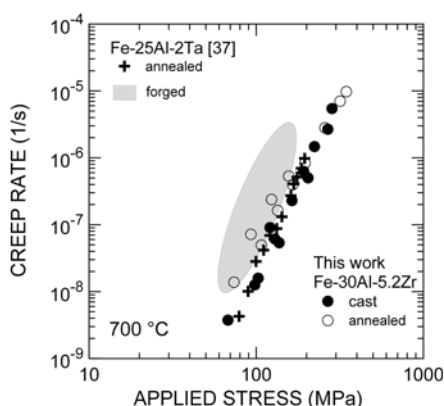Fig. 7. SEM images of the annealed alloy after creep at 900 °C.

Fig. 8. A comparison of measured creep rates at 700 °C with corresponding data of Fe-Al-Ta alloy.

900 °C. The solubility of Zr in Fe-Al is low and the microstructure of the cast alloy consists of Fe(Al) matrix and eutectic composed from lamellae of the λ_1-Laves phase and Fe(Al) (α/B2/D03). The eutectic decomposes into three-phase structure, $\alpha + \lambda_1 + \tau_1$, upon

annealing at 1000 °C for 50 h.

– The values of the stress exponent n can be explained by dislocation motion controlled by climb.

– The values of the activation energy in both cast and annealed alloy are slightly greater than the activation enthalpy of diffusion.

– Creep exposure at 900 °C for about 50 h is probably sufficient for attainment the three-phase structure because the same microstructure was observed after creep at 900 °C, in both as-cast and annealed states. In contrast, creep expositions at 650 and 700 °C did not influence the appearance of microstructure.

Acknowledgement

References

[1] Stoloff, N. S., Liu, C. T.: Intermetallics, 2, 1994, p. 75. doi:10.1016/0966-9795(94)90001-9
[2] Sauthoff, G.: Intermetallics. Weinheim, VCH Verlagsgesellschaft 1995. doi:10.1002/9783527615414
[3] Deevi, S. C., Sikka, V. K.: Intermetallics, 4, 1996, p. 357. doi:10.1016/0966-9795(95)00056-9
[4] Stoloff, N. S.: Mater. Sci. Engng. A, 258, 1998, p. 1. doi:10.1016/S0921-5093(98)00909-5
[5] Hotař, A., Kratochvíl, P., Hotař, V.: Kovove Mater., 47, 2009, p. 247.
[6] Alven, D. A.: Ph.D. Thesis. Troy, NY, Rensselaer Polytechnic Inst. 1997.
[7] McKamey, C. G., Maziasz, P. J., Jones, J. W.: J. Mater. Res., 7, 1992, p. 2089. doi:10.1557/JMR.1992.2089
[8] McKamey, C. G., Maziasz, P. J., Goodwin, G. M., Zacharia, T.: Mater. Sci. Engng. A, 174, 1994, p. 59. doi:10.1016/0921-5093(94)91112-6
[9] McKamey, C. G., Maziasz, P. J.: Intermetallics, 6, 1998, p. 303. doi:10.1016/S0966-9795(97)00104-0
[10] Morris, D. G., Gutierrez-Urrutia, I., Muñoz-Morris, M. A.: Scr. Mater., 57, 2007, p. 449. doi:10.1016/j.scriptamat.2007.05.038
[11] Khaple, S., Baligidad, R. G., Rao, S.: Mater. Sci. Technol., 23, 2007, p. 930. doi:10.1179/174328407X213134
[12] Matsumoto, N., Kaneno, Y., Takasugi, T.: Mater. Sci. Forum, 561–565, 2007, p. 395. doi:10.4028/www.scientific.net/MSF.561-565.395
[13] Machida, J., Kobayashi, S., Kaneno, Y., Takasugi, T.: Mater. Sci. Forum, 561–565, 2007, p. 399. doi:10.4028/www.scientific.net/MSF.561-565.399
[14] Kratochvíl, P., Málek, P., Cieslar, M., Hanus, P., Hakl, J., Vlasák, T.: Intermetallics, 15, 2007, p. 333. doi:10.1016/j.intermet.2006.07.005
[15] Cieslar, M., Karlík, M.: Mater. Sci. Engng. A, 462, 2007, p. 289. doi:10.1016/j.msea.2006.01.173
[16] Dobeš, F., Kratochvíl, P., Milička, K.: Strength Mater., 40, 2008, p. 106. doi:10.1007/s11223-008-0028-6
[17] Dobeš, F.: Scr. Mater., 59, 2008, p. 59. doi:10.1016/j.scriptamat.2008.02.021

[18] Karlík, M., Kratochvíl, P., Pešička, J., Vlasák, T.: Int. J. Mater. Res., *100*, 2009, p. 806. doi:10.3139/146.110120

[19] Karlík, M., Kubošová, A., Haušild, P., Prahl, J.: Kovove Mater., *46*, 2008, p. 77.

[20] Haušild, P., Karlík, M., Šíma, V., Alexander, D. T. L.: Mater. Sci. Technol., *27*, 2011, p. 1448. doi:10.1179/026708310X12738371693012

[21] Haušild, P., Siegl, J., Málek, P., Šíma, V.: Intermetallics, *17*, 2009, p. 608. doi:10.1016/j.intermet.2009.02.008

[22] Titran, R. H., Vedula, K. M., Anderson, G. G.: MRS Proceedings, *39*, 1984, p. 309. http://dx.doi.org10.1557/PROC-39-309

[23] Wasilkowska, A., Bartsch, M., Stein, F., Palm, M., Sztwiertnia, K., Sauthoff, G., Messerschmidt, U.: Mater. Sci. Engng. A, *380*, 2004, p. 9. doi:10.1016/j.msea.2004.04.005

[24] Wasilkowska, A., Bartsch, M., Stein, F., Palm, M., Sauthoff, G., Messerschmidt, U.: Mater. Sci. Engng. A, *381*, 2004, p. 1. doi:10.1016/j.msea.2004.04.039

[25] Stein, F., Palm, M., Sauthoff, G.: Intermetallics, *13*, 2005, p. 1275. doi:10.1016/j.intermet.2004.08.013

[26] Kratochvíl, P., Kejzlar, P., Král, R., Vodičková, V.: Intermetallics, *20*, 2012, p. 39. doi:10.1016/j.intermet.2011.08.007

[27] Dobeš, F., Kratochvíl, P.: Intermetallics, *43*, 2013, p. 142. doi:10.1016/j.intermet.2013.07.017

[28] Stein, F., Sauthoff, G., Palm, M.: Z. Metallkde., *95*, 2004, p. 469. doi:10.3139/146.017985

[29] Guo, C., Du, Z., Li, C., Zhang, B., Tao, M.: CALPHAD, *32*, 2008, p. 637. doi:10.1016/j.calphad.2008.08.007

[30] Rigaud, V., Sundman, B., Daloz, D., Lesoult, G.: CALPHAD, *33*, 2009, p. 442. doi:10.1016/j.calphad.2009.05.003

[31] Stein, F., Palm, M.: Int. J. Mater. Res., *98*, 2007, p. 580. doi:10.3139/146.101512

[32] Rees, D. W. A.: Basic Engineering Plasticity: An Introduction with Engineering and Manufacturing Applications. Boston, MA, Elsevier 2006, p. 279.

[33] Eggersmann, M., Mehrer, H.: Philos. Mag. A, *80*, 2000, p. 1219. doi:10.1080/01418610008212112

[34] Larikov, L. N., Geichenko, V. V., Faľchenko, V. M.: Diffusion Processes in Ordered Alloys. New Delhi, Oxonian Press 1981.

[35] Sherby, O. D., Burke, P. M.: Progress Mater. Sci., *13*, 1967, p. 323. doi:10.1016/0079-6425(68)90024-8

[36] Mohamed, F. A., Langdon, T. G.: Acta Metall., *22*, 1974, p. 779. doi:10.1016/0001-6160(74)90088-1

[37] Risanti, D. D., Sauthoff, G.: Intermetallics, *19*, 2011, p. 1727. doi:10.1016/j.intermet.2011.07.008